WILEY | Hindawi

Research Article

A Detailed Study of a Fractal-Fractional Transmission Dynamical Model of Viral Infectious Disease with Vaccination

Kamal Shah [ID],[1,2] **Muhammad Sinan** [ID],[3] **Thabet Abdeljawad** [ID],[1,4] **M.A. El-Shorbagy** [ID],[5,6] **Bahaaeldin Abdalla** [ID],[1] and **Marwan S. Abualrub**[7]

[1]*Department of Mathematics and Sciences, Prince Sultan University, Riyadh 11586, Saudi Arabia*
[2]*Department of Mathematics, University of Malakand, Chakdara Dir (L), Khyber Pakhtunkhwa 18000, Pakistan*
[3]*School of Mathematical Sciences, University of Electronic Science and Technology of China, Chengdu 611731, China*
[4]*Department of Medical Research, China Medical University, Taichung 40402, Taiwan*
[5]*Department of Mathematics, College of Science and Humanities in Al-Kharj, Prince Sattam Bin Abdulaziz University, Al-Kharj 11942, Saudi Arabia*
[6]*Department of Basic Engineering Science, Faculty of Engineering, Menoufia University, Shebin El-Kom 32511, Egypt*
[7]*Mathematics Department (Prep.Programm) Faculty of Science, Khalifa University, P.O. Box 127788, Abu Dhabi, UAE*

Correspondence should be addressed to Thabet Abdeljawad; tabdeljawad@psu.edu.sa

This article is devoted to investigate a mathematical model consisting on susceptible, exposed, infected, quarantined, vaccinated, and recovered compartments of COVID-19. The concerned model describes the transmission mechanism of the disease dynamics with therapeutic measures of vaccination of susceptible people along with the cure of the infected population. In the said study, we use the fractal-fractional order derivative to understand the dynamics of all compartments of the proposed model in more detail. Therefore, the first model is formulated. Then, two equilibrium points disease-free (DF) and endemic are computed. Furthermore, the basic threshold number is also derived. Some sufficient conditions for global asymptotical stability are also established. By using the next-generation matrix method, local stability analysis is developed. We also attempt the sensitivity analysis of the parameters of the proposed model. Finally, for the numerical simulations, the Adams–Bashforth method is used. Using some available data, the results are displayed graphically using various fractal-fractional orders to understand the mechanism of the dynamics. In addition, we compare our numerical simulation with real data in the case of reported infected cases.

1. Introduction

Various viral infectious diseases have greatly affected human life in the past. Some famous viral infectious diseases were known as swine flu, influenza, SARs, MERs, etc. Recently, coronavirus disease 2019 (COVID-19) has greatly affected human life all over the world. The said infection has been reported for the first time in Wuhan, China, in December 2019. After three months, the disease took the form of a pandemic which was announced by the WHO in April 2020 (see [1]). Recent estimates issued by the WHO showed that the full death toll associated directly or indirectly with the COVID-19 pandemic between 1 January 2020 and 31 December 2021 was approximately 14.9 million (see details in [2]). Approximately, more than six hundred million people have got infections (see [3, 4]). Since the outbreak surrounded the whole globe, each nation in the world has taken its own measures. Some countries have imposed a strict curfew and precautionary measures including wearing face masks, keeping social distance, and avoiding large gatherings. Europe has been seriously affected along with USA, Brazil, Iran, and India. Initially it was reported that the disease has been transmitted from some animals to humans because the virus was first identified in a man who was working in a fish market. After that, various researchers proved that bats are not a unique source and the mentioned

disease may be transmitted from other animals, person to person, and dogs (see [5, 6]).

Epidemiology is the most important branch of medical science and it has been very well developed in recent times. In the said area, various infectious diseases are investigated for treatment, controlling, curing, etc. Moreover, virology is a sub-branch, particularly dealing with virus and their transmitted diseases. Here, we remark that infectious diseases are investigated via various tools and methods. Bio-mathematics and bio-informatics engineering have attracted researchers recently more than in the past. It is worth mentioning that mathematical models are powerful tools to describe various real-world problems. Therefore, modeling infectious diseases is a hot area of research at the present time. In the said area, the dynamics of various infectious diseases are explained by using various differential or integral equations (some studies we refer to as [7–9]). Mathematical models help us to investigate various diseases for prediction and controlling procedures, to save society from great loss. Inspired by the aforesaid importance of mathematical models, researchers have formulated various real-world infectious diseases, we refer some as (see [10–15] and [16]). COVID-19 has been transmitted nearly to every part of the Earth and affected every nation of the world. The health conditions and economical situation of well-developed counties have been disturbed very well. In recent times, the world needs effective medication for the said diseases to save the lives of people. In this regard, great trials have been performed on vaccine preparation so far (for such detail, we refer [17]). Some authors have identified that COVID-19 vaccination in low and middle-income nations is extremely cost-effective and even price-saving (see [18]). The infection can be minimized all over the world by providing a vaccine to all nations of the world without any obstacles. Because by doing so, we can secure the next generation from the deadly virus. Moreover, some measures, like treatment, and vaccination, nonpharmaceutical precautionary measures, for instance, quarantine of confirmed cases, isolation, face masks, hand washing, social distancing, and avoiding gathering, should be imposed to reduce the transmission. Currently, some versions of the virus have been identified which indicate a new threat to human life. However, researchers have proved that the currently available vaccine is useful in medication. Moreover, it has been proved that vaccinated people if infected can easily be recovered compared to nonvaccinated people. However, this is not a permanent solution. Therefore, preparing proper vaccines and their availability without any bound in every society at a low price will be the best solution. Although, in some people, the vaccine has shown some adverse reactions. However, with the passage of time, things will become relaxed.

Most real-world problems are nonlinear in nature. In the same line, most epidemiological processes or phenomena are modeled in the form of nonlinear equations under traditional order derivatives or difference equations. As ordinary differential operators are local in nature and cannot produce the global dynamical behavior of the phenomenon, researchers are increasingly using fractional order derivatives in mathematical models (for instance, see

[19–22], and [23]). A significant amount of work has been performed in this regard. Some well-known studies are referred here as [24–28], and [26]. In current times, in almost every discipline including fluid dynamics, bio-engineering, control theory, epidemiology, and rheology, the concept of fractional calculus is increasingly used to study various processes and phenomenons (see [29–32]). On the other hand, the said area has been exploited in engineering sides also recently (see [33–35]). Here it is worth mentioning that fractal geometry can be used as a powerful tool to investigate complex phenomena and every irregular picture in nature properly. Furthermore, fractal curves and surfaces are treated by using fractal dimensions to investigate their roughness. Because natural graphs are analyzed by using fractal interpolation (see some details in [36]). In previous times, due to the complex nature of fractional calculus, researchers have studied fractal surfaces through classical integer order calculus. Recently, many researchers have used the fractal-fractional order concept to investigate various real-world problems relating to epidemiology and physics, and chemical sciences. Here, we refer to some good work as [37].

Due to the ability to explain complex nature and preserve memory concepts, the idea of fractal calculus is widely used in the mathematical modeling of various diseases (details can be seen in [38]). For dealing with problems involving the fractal-fractional order derivatives, the traditional analytical and numerical techniques have been updated (see [39, 40], and [41]). Moreover, various numerical methods used for fractional derivatives have been applied to treat fractal-fractional problems. For instance, Adams–Bashforth procedure has been updated for dealing classical and fractal-fractional order problems (see [42–49]). Also, some authors have investigated other infectious diseases models like [50–54], and [55]. Authors [56] studied the psychological effects of staying home due to the COVID-19 pandemic. For instance, the authors applied a novel fractal-fractional order operator to the mathematical model of optimal control for malaria, where the derivative is defined in the Caputo sense. Two control variables have been introduced, as well as the necessary optimality condition in order to minimize the low-risk and high-risk infectious humans. Furthermore, the optimal control has been studied and results were simulated using a numerical scheme (see [57, 58]). In the same fashion, the author [59] proposed a compartmental mathematical model to acquire a better understanding of COVID-19's future dynamics. The problem has been described as a highly nonlinear coupled system of classical order ODEs, which has then been generalized using the fractal-fractional derivative with the Mittag-Leffler kernel. For recent work on fractional order models, see [60], and [61]. Moreover, the boundedness and non-negativity of the model have been established as well. Here it should be kept in mind that authors [62] studied the backward bifurcation of a vaccination model with nonlinear incidence. Authors [63] studied a COVID-19 model. Authors [64] studied some stability results in control process by using fractional derivative. For more applications of fractional derivative, we refer [65]. Using mathematical models and the concept of fractional calculus, we refer some
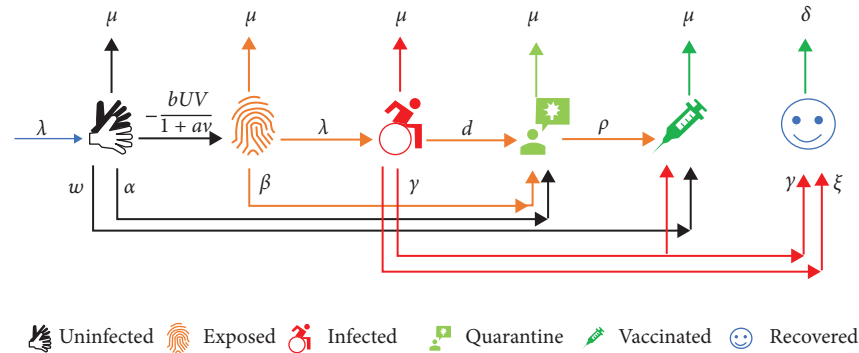
Figure 1: Compartment diagram of COVID–19.

recent work like [66–69], and [70]. Also authors investigated a fractional order model for HIV infection in [71].

Motivated by the aforesaid discussion, we formulate the proposed model under the fractal-fractional order derivative. We investigate the proposed mathematical model with the vaccinated class by considering the available therapeutic measures, vaccination of susceptible, and curing of infected/hospitalized people. Our considered model involves some important epidemiological and biological features of the said disease like inhibitory effect, death rates due to infection and nature, birth rate, and different vaccination rates. A flow chart of our study is given in Figure 1.

Considering the compartmental diagram, the model is formulated as

$$
\left.\begin{aligned}
{}^{\mathbf{FFP}}_{0}\mathscr{D}^{\upsilon,\pi}U(t) &= \Lambda - \frac{bUV}{1+aV} - (\omega + \mu + \alpha)U, \\[2mm]
{}^{\mathbf{FFP}}_{0}\mathscr{D}^{\upsilon,\pi}V(t) &= \frac{bUV}{1+aV} - (\lambda + \mu + \beta)V, \\[2mm]
{}^{\mathbf{FFP}}_{0}\mathscr{D}^{\upsilon,\pi}W(t) &= \lambda V - (\mu + \xi + \gamma + d)W, \\[2mm]
{}^{\mathbf{FFP}}_{0}\mathscr{D}^{\upsilon,\pi}Q(t) &= \alpha U + \beta V + dW - (\mu + \rho)Q, \\[2mm]
{}^{\mathbf{FFP}}_{0}\mathscr{D}^{\upsilon,\pi}X_v &= \omega U + \rho Q + \gamma W - \mu X_v, \\[2mm]
{}^{\mathbf{FFP}}_{0}\mathscr{D}^{\upsilon,\pi}Y &= \xi W + \gamma W - \delta Y.
\end{aligned}\right\}. \quad (1)
$$

Symbols involved in model (1) are described in Table 1. Also, the nomenclature and their dimensions are described in Table 2.

Using various tools of mathematical analysis, we establish global and local stability. The said analysis is established by the Lyapunov method and next-generation matrix method. Moreover, by using the Pontryagin maximum principle, we develop some results about the optimal control procedure. Furthermore, sensitivity analysis is also investigated about the parameters involved in our proposed model. Some results for numerical stability are derived by

Table 1: The compartments and their description involved in model (1) with initial values.

Variables	Physical representation	Initial values
U	The uninfected class	2500
V	The exposed class	20
W	The infected class	70
Q	The quarantine class	3
X_v	The vaccinated class	10
Y	The recovered class	20

Table 2: The parameters and their description involved in model (1).

Variables	Physical representation	Dimension
Λ	Birth rate	month^{-1}
ξ	COVID-19 death rate	month^{-1}
μ	Natural death rate	month^{-1}
a	Inhibitory effect rate	month^{-1}
b	Saturation constant	month^{-1}
β	Infection rate from exposed class	month^{-1}
α	Rate of quarantine from susceptible class	month^{-1}
β	Rate of quarantine from exposed class	month^{-1}
d	Quarantine from infected class	month^{-1}
ω	Vaccination rate of susceptible	month^{-1}
γ	Vaccination rate of infected	month^{-1}
ρ	Vaccination rate of quarantine	month^{-1}

using the Ulam–Hyers concept. We also perform numerical simulation for our considered model by using a numerical method based on the Adams–Bashforth method to investigate multiphase behaviors under various fractal-fractional order derivatives. Here, we remark that multistep methods are increasingly used because these procedures are more efficient than the earlier methods like the Euler method. Moreover, the derivation of the Adams–Bashforth method can be performed in a number of ways. By using numerical interpolation and numerical integration, one can easily derive the aforesaid method. Therefore, we use the aforesaid scheme to simulate our model by using some numerical values of the parameters and initial data given in Table 1. A graphical presentation of some real data and discussion are provided.

2. Preliminaries

In this section, we recall the fractional-fractional operators as given below.

Definition 1 (see [61]). Let the function v be differentiable in the opened interval (a, b), then the fractional-fractional derivative with v and π are fractal and fractional orders, respectively, in the Caputo sense with power law is given as

$$\,_{a}^{\text{FFP}}\mathscr{D}\,_{t}^{v,\pi} v(t) = \frac{1}{\Gamma[m-\pi]} \int_{a}^{t} \frac{dv(\xi)}{d\xi^{v}} (t-\xi)^{m-\pi-1} d\xi,$$

$$m - 1 < \pi \leq m, 0 < m - 1 < v \leq m, \qquad (2)$$

$$\frac{dv(\xi)}{d\xi^{v}} = \lim_{t-\xi} \frac{v(t) - v(\xi)}{t^{v} - \xi^{v}}.$$

Here, v is continuous over the interval (a, b).

Definition 2 (see [61]). The fractal-fractional integral of a function v with fractal order $v > 0$ and fractional order $\pi > 0$ is defined as

$$\,_{0}^{\text{FFP}}\mathscr{I}\,_{t}^{v,\pi} v(t) = \frac{v}{\Gamma(\pi)} \int_{0}^{t} \xi^{\lambda-1} v(\xi) (t-\xi)^{\pi-1} d\xi, \qquad (3)$$

where v is continuous over the interval (a, b).

Definition 3. Consider the fractal-fractional nonlinear ODE, such that

$$\,_{0}^{\text{FFP}}\mathscr{D}\,^{v,\pi} g(t) = v(t, u(t)), \text{with} g(0) = g_{0}. \qquad (4)$$

From [45], the resultant Adams–Bashforth scheme for (4) can be written as

$$g(l+1) = g_{0} + \frac{v\hbar^{\pi}}{\Gamma(\pi+2)} \sum_{j=0}^{f} \left[t_{(j)}^{v-1} g\left(w_{(j)}, t_{j}\right) \times \left((f+1-j)^{v}(f-j+2+v) - (f-j)^{v}(f-j+2+2v)\right) \right.$$

$$\left. - t_{(j-1)}^{v-1} v\left(w_{(j-1)}, t_{(j-1)}\right) \left((f+1-j)^{v} + 1 - (f-j)^{v}(f-j+1+v)\right) \right]. \qquad (5)$$

3. Equilibrium Points and Stability

This section is enriched with various stability results and equilibrium points.

3.1. Equilibrium Points. The disease-free equilibrium point is given by

$$\mathscr{E}^{0} = \left(U^{0}, 0, 0, 0, X_{v}^{0}, 0\right), \qquad (6)$$

where

$$U^{0} = \frac{\lambda}{(\omega + \mu + \alpha)},$$
$$X_{v}^{0} = \frac{\omega}{\mu(\omega + \mu + \alpha)}, \qquad (7)$$

while the positive disease-endemic equilibrium is computed in terms of one class such that

$$\mathscr{E}^{*} = \left(U^{*}, V^{*}, W^{*}, Q^{*}, X_{V}^{*}, Y^{*}\right), \qquad (8)$$

where

$$V^{*} = \frac{U^{*}(\omega + \mu + \alpha) - \lambda}{\lambda + \mu + \beta},$$

$$W^{*} = \frac{\lambda U^{*}(\omega + \mu + \alpha) - \lambda^{2}}{(\mu + \xi + \gamma + d)(\lambda + \mu + \beta)},$$

$$Q^{*} = \frac{1}{\mu + \rho} \left[\alpha U^{*} + \frac{\beta U^{*}(\omega + \mu + \alpha) - \lambda}{\lambda + \mu + \beta} + \frac{d\lambda\, U^{*}(\omega + \mu + \alpha) - \lambda^{2}}{(\mu + \xi + \gamma + d)(\lambda + \mu + \beta)} \right],$$

$$X_{V}^{*} = \frac{\rho}{\mu(\mu + \rho)} \left[\frac{\beta U^{*}(\omega + \mu + \alpha) - \lambda}{(\lambda + \mu + \beta)} + \frac{d\lambda\, U^{*}(\omega + \mu + \alpha) - \lambda^{2}}{(\mu + \xi + \gamma + d)(\lambda + \mu + \beta)} + \alpha U^{*} \right],$$

$$Y^{*} = \frac{\xi + \gamma}{\delta} \left[\frac{\lambda U^{*}(\omega + \mu + \alpha) - \lambda^{2}}{(\mu + \xi + \gamma + d)(\lambda + \mu + \beta)} \right].$$

$$\qquad (9)$$

3.2. Basic Reproduction Number

$$\frac{\mathrm{d}Z}{\mathrm{d}t}\Big|_{E^0} = F - V. \tag{10}$$

The nonlinear and linear terms of the infected classes in matrices F and V, respectively, are given as

$$F = \begin{pmatrix} \dfrac{UVb}{Va+1} \\ 0 \\ 0 \\ 0 \end{pmatrix}, \tag{11}$$

$$V = \begin{pmatrix} V(\beta + \lambda + \mu) \\ W(d + \gamma + \mu + \xi) - V\lambda \\ Q(\mu + \rho) - V\beta - W\,d - U\alpha \\ X_v\mu - Q\rho - U\omega - W\gamma \end{pmatrix}.$$

Thus, the nonzero and largest eigenvalue is the basic reproduction number $\mathscr{R}_0$, which is

$$R_0 = \frac{b\lambda}{(\omega + \mu + \alpha)(\beta + \lambda + \mu)}. \tag{14}$$

3.3. Stability Analysis

Lemma 1 (see [60]). *Let A be a 2×2 matrix, then the eigenvalues of the matrix A are negative in real part if $trace(A) < 0$, and $det(A) > 0$.*

Now, the Jacobian matrix of F and V is given by

$$F = \begin{pmatrix} U^0 b & 0 & 0 & 0 \\ 0 & 0 & 0 & 0 \\ 0 & 0 & 0 & 0 \\ 0 & 0 & 0 & 0 \end{pmatrix},$$

$$V = \begin{pmatrix} \beta + \lambda + \mu & 0 & 0 & 0 \\ -\lambda & d + \gamma + \mu + \xi & 0 & 0 \\ -\beta & -d & \mu + \rho & 0 \\ 0 & -\gamma & -\rho & \mu \end{pmatrix}. \tag{12}$$

Calculating the inverse of matrix V and the next-generation matrix $G(E^0)$, such that

$$V^{-1} = \begin{pmatrix} \dfrac{1}{\beta + \lambda + \mu} & 0 & 0 & 0 \\[2ex] \dfrac{\lambda}{(\beta + \lambda + \mu)(d + \gamma + \mu + \xi)} & \dfrac{1}{d + \gamma + \mu + \xi} & 0 & 0 \\[2ex] \dfrac{\beta\,d + \beta\gamma + \beta\mu + d\lambda + \beta\xi}{(\mu + \rho)(\beta + \lambda + \mu)(d + \gamma + \mu + \xi)} & \dfrac{d}{(\mu + \rho)(d + \gamma + \mu + \xi)} & \dfrac{1}{\mu + \rho} & 0 \\[2ex] \dfrac{\beta\,d\rho + \beta\gamma\rho + \gamma\lambda\mu + \beta\mu\rho + d\lambda\,\rho + \gamma\lambda\rho + \beta\rho\xi}{\mu(\mu + \rho)(\beta + \lambda + \mu)(d + \gamma + \mu + \xi)} & \dfrac{\gamma\mu + d\rho + \gamma\rho}{\mu(\mu + \rho)(d + \gamma + \mu + \xi)} & \dfrac{\rho}{\mu(\mu + \rho)} & \dfrac{1}{\mu} \end{pmatrix}. \tag{13}$$

Theorem 1. *The COVID-19 model at the disease-free equilibrium point E^0, is locally asymptotically stable if $\mathscr{R}_0 < 1$, otherwise unstable.*

Proof 1. The Jacobian matrix of system (1) at disease-free equilibrium point E^0 is given by

$$J(E^0) = \begin{pmatrix} -\alpha - \mu - \omega & -U^0 b & 0 & 0 & 0 & 0 \\ 0 & U^0 b - \lambda - \mu - \beta & 0 & 0 & 0 & 0 \\ 0 & \lambda & -d - \gamma - \mu - \xi & 0 & 0 & 0 \\ \alpha & \beta & d & -\mu - \rho & 0 & 0 \\ \omega & 0 & \gamma & \rho & -\mu & 0 \\ 0 & 0 & \gamma + \xi & 0 & 0 & -\delta \end{pmatrix}. \tag{15}$$

Following the characteristic equation of the Jacobian matrix (14), we have

$$(\varepsilon + \delta)(\varepsilon + \mu)(\varepsilon + (\mu + \rho))(\varepsilon + (d + \gamma + \mu + \xi))$$
$$(\varepsilon + (\alpha + \mu + \omega))(\varepsilon - (\lambda + \mu + \beta - U^0 b)) = 0. \qquad (16)$$

Thus, the eigenvalues of the characteristic (16) are given by

$$\left.\begin{array}{l} \varepsilon_1 = -\delta, \\ \varepsilon_2 = -\mu, \\ \varepsilon_3 = -(\mu + \rho), \\ \varepsilon_4 = -(d + \gamma + \mu + \xi), \\ \varepsilon_5 = -(\alpha + \mu + \omega), \\ \varepsilon_6 = (\lambda + \mu + \beta)[R_0 - 1]. \end{array}\right\} . \qquad (17)$$

As a result, all eigenvalues of the Jacobian matrix (15) are negative for $(\lambda + \mu + \beta)[R_0 - 1] < 0$, such that $R_0 < 1$. Hence, model (1) is locally asymptotically stable around a disease-free equilibrium point. □

Theorem 2. *The COVID-19 model at the disease-endemic equilibrium point E^* is locally asymptotically stable if $R_0 > 1$, otherwise unstable.*

Proof 2. The Jacobian matrix of system (1) at disease-endemic equilibrium point E^* is given by

$$J_1(E^*) = \begin{pmatrix} -(\alpha + \mu + \omega) - \dfrac{V^* b}{V^* a + 1} & -\dfrac{U^* b}{(V^* a + 1)^2} & 0 & 0 & 0 & 0 \\[2ex] \dfrac{V^* b}{V^* a + 1} & \dfrac{U^* b}{V^* a + 1} - (\lambda + \mu + \beta) - \dfrac{U^* V^* ab}{(V^* a + 1)^2} & 0 & 0 & 0 & 0 \\[2ex] 0 & \lambda & -(d + \gamma + \mu + \xi) & 0 & 0 & 0 \\[2ex] \alpha & \beta & d & -(\mu + \rho) & 0 & 0 \\[2ex] \omega & 0 & \gamma & \rho & -\mu & 0 \\[2ex] 0 & 0 & \gamma + \xi & 0 & 0 & -\delta \end{pmatrix}, \qquad (18)$$

$$(\varepsilon + \delta)(\varepsilon + \mu)(\varepsilon + (\mu + \rho))(\varepsilon + (d + \gamma + \mu + \xi))(\varepsilon + (\alpha + \mu + \omega)) = 0.$$

Thus, eigenvalues of the characteristic (16) are given by

$$\left.\begin{array}{l} \varepsilon_1 = -\delta, \\ \varepsilon_2 = -\mu, \\ \varepsilon_3 = -(\mu + \rho), \\ \varepsilon_4 = -(d + \gamma + \mu + \xi). \end{array}\right\} . \qquad (19)$$

However, the reduced matrix takes the form

$$J_2(E^*) = \begin{pmatrix} -(\alpha + \mu + \omega) - \dfrac{V^* b}{V^* a + 1} & -\dfrac{U^* b}{(V^* a + 1)^2} \\[3ex] \dfrac{V^* b}{V^* a + 1} & \dfrac{U^* b}{V^* a + 1} - (\lambda + \mu + \beta) - \dfrac{U^* V^* ab}{(V^* a + 1)^2} \end{pmatrix} . \qquad (20)$$

The matrix (20) possesses negative eigenvalues if the trace $(J_2(E^*))$ is negative and determinant $(J_2(E^*))$ is positive, such that

$$\text{Trace}\,(J_2(E^*)) = -(\alpha + \mu + \omega) - \frac{V^*b}{V^*a + 1} - (\lambda + \mu + \beta) - \frac{U^*b}{1 + aV^*}\left(\frac{aV^*}{1 + aV^*} - 1\right) < 0,$$

$$\text{Determinant}\,(J_2(E^*)) = \frac{b}{(1 + aV^*)}\left((\alpha + \mu + \omega) + \frac{V^*b}{V^*a + 1} + (\lambda + \mu + \beta) + \frac{U^*b}{1 + aV^*}\left(\frac{aV^*}{1 + aV^*} - 1\right)\right)\left(\frac{U^*}{1 + aV^*} - V\right) > 0.$$

(21)

The determinant is positive if $U^*b/V^*a + 1 > U^*V^*ab/(V^*a + 1)^2$. Hence, model (1) is locally asymptotically stable around the disease-endemic equilibrium point with negative eigenvalues of $J_1(E^*)$ and $R_0 > 1$. □

4. Globally Asymptotical Stability

Theorem 3. *For nonautonomous fractional order system, let $\overline{a} = 0$ be an equilibrium point, such that*

$$^{\text{FFP}}D_t^{v,\pi}\overline{a}(t) = g(t, \overline{a}), \overline{a}(t_0) = \overline{a}_0.$$

(22)

Let $\Lambda \subseteq R^n$ be a domain which contains $\overline{a} = 0$. Let $\mathscr{L}(t, \overline{a}) \colon [t_0, \infty] \times \Lambda \longrightarrow R$ be a continuously differentiable function such that $\overline{w}_1(\overline{a}) \le \overline{v}(t, \overline{a}) \le \overline{w}_2(u)$ and $^{\text{FFP}}D_t^v\mathscr{L}(t, \overline{a}) \le -\overline{w}_3(\overline{a})$, for $t \ge 0, \overline{a} \in \Omega$, where continuous positive definite functions $\overline{w}_1(\overline{a}), \overline{w}_2(\overline{a})$, and $\overline{w}_3(\overline{a})$ on Λ and $\mathscr{L}$ is Lyapunov candidate function, then, $\overline{a} = 0$, is globally asymptotically stable.

Lemma 2. *For the fractal-fractional order, we use the lemma defined for fractional order ODE from [42, 60]. At any instant of time $t \ge t_0$, assume a continuous differentiable function $\overline{a}$ as*

$$\frac{1}{2}\,^{\text{FFP}}D_t^{v,\pi}\overline{a}^2(\mathbf{t}) \le\,^{\text{FFP}}D_t^{v,\pi}\overline{a}(t), \text{for all}\, v, \pi \in (0, 1).$$

(23)

Theorem 4. *Equilibrium point E^* is globally asymptotically stable.*

Proof 3. We consider the quadratic Lyapunov function to derive the Lyapunov candidate function for fractional order differential equation.

$$\mathscr{L}(\overline{a}_1, \overline{a}_2, \overline{a}_3, \ldots, \overline{a}_n) = \sum_{k=1}^{n}\frac{s_k}{2}(\overline{a}_k(t) - \overline{a}^*)^2.$$

(24)

We define the Lyapunov candidate function as

$$\mathscr{L}(U(t), V(t), W(t), Q(t), X_v(t), Y(t)) = \frac{1}{2}(U(t) - U^*) + \frac{1}{2}(V(t) - V^*) + \frac{1}{2}(W(t) - W^*) + \frac{1}{2}(Q(t) - Q^*)$$

$$+ \frac{1}{2}(X_v(t) - X_v^*) + \frac{1}{2}(Y(t) - Y^*).$$

(25)

The linearity property is given as

$$^{\text{FFP}}_{0}D_t^{v,\pi}\mathscr{L}(U(t), V(t), W(t), Q(t), X_v(t), Y(t))$$

$$= \frac{1}{2}\left[^{\text{FFP}}_{0}D_t^{v,\pi}(U(t) - U^*) +\,^{\text{FFP}}_{0}D_t^{v,\pi}(V(t) - V^*) +\,^{\text{FFP}}_{0}D_t^{v,\pi}(W(t) - W^*) +\,^{\text{FFP}}_{0}D_t^{v,\pi}(Q(t) - Q^*) +\,^{\text{FFP}}_{0}D_t^{v,\pi}(X_v(t) - X_v^*) +\,^{\text{FFP}}_{0}D_t^{v,\pi}(Y(t) - Y^*)\right].$$

(26)

Using Lemma 2, we have

$$
\begin{aligned}
{}_{0}^{\text{FFP}}D_{t}^{\upsilon,\pi}\mathscr{L}(U(t),V(t),W(t),Q(t),X_{\nu}(t),Y(t)) &= {}_{0}^{\text{FFP}}D_{t}^{\upsilon,\pi}(U(t)-U^{*}) + {}_{0}^{\text{FFP}}D_{t}^{\upsilon,\pi}(V(t)-V^{*})\\
&\quad + {}_{0}^{\text{FFP}}D_{t}^{\upsilon,\pi}(W(t)-W^{*}) + {}_{0}^{\text{FFP}}D_{t}^{\upsilon,\pi}(Q(t)-Q^{*}) + {}_{0}^{\text{FFP}}D_{t}^{\upsilon,\pi}(X_{\nu}(t)-X_{\nu}^{*})\\
&\quad + {}_{0}^{\text{FFP}}D_{t}^{\upsilon,\pi}(Y(t)-Y^{*}) \le \lambda - \mu(N(t)-N^{*}) - \mu(Y(t)-Y^{*}) - \delta(Y(t)-Y^{*}),
\end{aligned} \tag{27}
$$

which further implies that

$$
{}_{0}^{\text{FFP}}D_{t}^{\upsilon,\pi}\mathscr{L}(U(t),V(t),W(t),Q(t),X_{\nu}(t),Y(t)) \le \lambda - \mu(N(t)-N^{*}) - \mu(Y(t)-Y^{*}) - \delta(Y(t)-Y^{*}). \tag{28}
$$

$\square$

4.1. Global Stability at Disease-Free Equilibrium Point E^{0}.
Using disease-free equilibrium point, $N^{0} = (\Lambda/\mu)$ in the last equation of the proposed model, one has

$$
{}_{0}^{\text{FFP}}D_{t}^{\upsilon,\pi}\mathscr{L}(U(t),V(t),W(t),Q(t),X_{\nu}(t),Y(t))
$$

$$
\le \lambda - \mu(N(t)-N^{0}) - \mu(Y(t)-Y^{0}) - \delta(Y(t)-Y^{0}) \tag{29}
$$

$$
\le \lambda - \mu\left(N(t)-\frac{\lambda}{\mu}\right) - Y(t)(\mu+\delta) \le -\overline{w}(\overline{a}(t)).
$$

The last inequality (29) is negative if $\overline{w}(\overline{a}(t)) > 0$, such that if $\lambda > \mu(N(t) - \lambda/\mu) + Y(t)(\mu+\delta)$. Hence, model (1) is globally asymptotically stable around disease-free equilibrium point, E^{0} with N^{0}.

4.2. Global Stability at Disease-Endemic Equilibrium Point E^{*}.
For global stability around disease-endemic equilibrium point E^{*} and N^{*}, we have

$$
\begin{aligned}
&{}_{0}^{\text{FFP}}D_{t}^{\upsilon,\pi}\mathscr{L}(U(t),V(t),W(t),Q(t),X_{\nu}(t),Y(t))\\
&\le \lambda - \mu(N(t)-N^{*}) - \mu(Y(t)-Y^{*}) - \delta(Y(t)-Y^{*}),
\end{aligned} \tag{30}
$$

where

$$
\begin{aligned}
N^{*} &= \frac{\lambda - Y^{*}(\mu+\delta)}{\mu},\\
Y^{*} &= \frac{\xi+\gamma}{\delta}\left[\frac{\lambda U^{*}(\omega+\mu+\alpha)-\lambda^{2}}{(\mu+\xi+\gamma+d)(\lambda+\mu+\beta)}\right].
\end{aligned} \tag{31}
$$

From (30) and (31), we obtain

$$
\begin{aligned}
&{}_{0}^{\text{FFP}}D_{t}^{\upsilon,\pi}\mathscr{L}(U(t),V(t),W(t),Q(t),X_{\nu}(t),Y(t) \le 2\lambda - \mu N(t))\\
&\quad - Y^{*}(\mu+\delta),\\
&\quad - Y(t)(\mu+\delta) - \frac{\xi+\gamma}{\delta}\left[\frac{\lambda U^{*}(\omega+\mu+\alpha)-\lambda^{2}}{(\mu+\xi+\gamma+d)(\lambda+\mu+\beta)}\right](\mu+\delta),\\
&\le -\overline{w}(\overline{a}(t)).
\end{aligned} \tag{32}
$$

The last inequality (32) is negative if $\overline{w}(\overline{a}(t))$ is positive such that, if $2\lambda > \mu N(t) + Y^{*}(\mu+\delta) + Y\ \ (t)(\mu+\delta) + \xi + \gamma/\delta[\lambda U^{*}(\omega+\mu+\alpha) - \lambda^{2}/(\mu+\xi+\gamma+d)(\lambda+\mu+\beta)](\mu+\delta)$. Hence, model (1) is globally asymptotically stable around disease-endemic equilibrium point, E^{*} with N^{*}.

5. Sensitivity Analysis

$$
\mathbb{S}_{p}^{R_{0}} = \frac{p}{R_{0}}\left[\frac{\partial R_{0}}{\partial p}\right]. \tag{33}
$$

Now, according to the (33) relation, we have

$$
\left.\begin{aligned}
S_{\nu}^{R_{0}} &= \frac{b}{R_{0}}\left[\frac{\lambda}{(\beta+\lambda+\mu)(\alpha+\mu+\omega)}\right] > 0,\\
S_{\tau}^{R_{0}} &= \frac{\lambda}{R_{0}}\left[\frac{b(\beta+\mu)}{(\beta+\lambda+\mu)^{2}(\alpha+\mu+\omega)}\right] > 0,\\
S_{\vartheta}^{R_{0}} &= -\frac{\omega}{R_{0}}\left[\frac{b\lambda}{(\beta+\lambda+\mu)(\alpha+\mu+\omega)^{2}}\right] < 0,\\
S_{\chi}^{R_{0}} &= -\frac{\mu}{R_{0}}\left[\frac{b\lambda(\alpha+\beta+\lambda+2\mu+\omega)}{(\beta+\lambda+\mu)^{2}(\alpha+\mu+\omega)^{2}}\right] < 0,\\
S_{\varrho_{1}}^{R_{0}} &= -\frac{\alpha}{R_{0}}\left[\frac{b\lambda}{(\beta+\lambda+\mu)(\alpha+\mu+\omega)^{2}}\right] < 0,\\
S_{\upsilon}^{R_{0}} &= -\frac{\beta}{R_{0}}\left[\frac{b\lambda}{(\beta+\lambda+\mu)^{2}(\alpha+\mu+\omega)}\right] < 0.
\end{aligned}\right\} \tag{34}
$$

Here, in Figures 2–7, we have described graphically the dynamics of sensitivity analysis of various parameters, respectively.

Furthermore, we present Table 3 for the sensitivity index of each parameter associated with R_{0} based on system (34).

Considering Table 3, the change in the value of each parameter in the basic reproduction number causes an increase or decrease in the value of the basic reproduction number R_{0}. Hence, it directly affects the spread in the population while keeping the values of the remaining
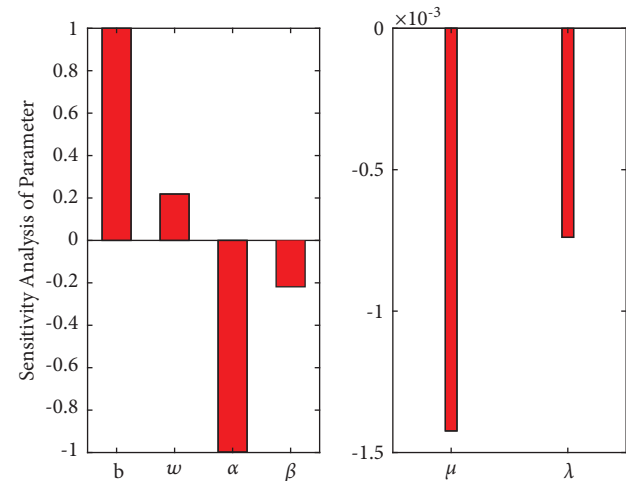
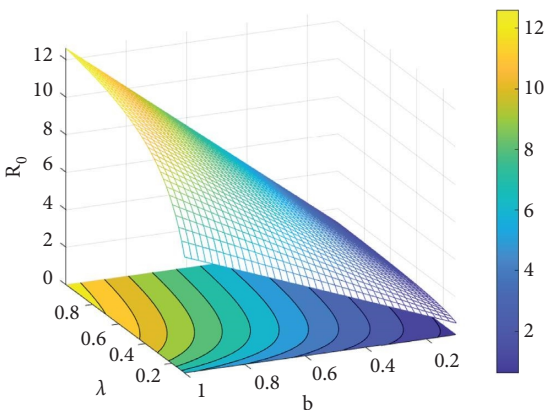FIGURE 2: The dynamics of sensitivity analysis based on R_0 with respect to each parameter associated with R_0.
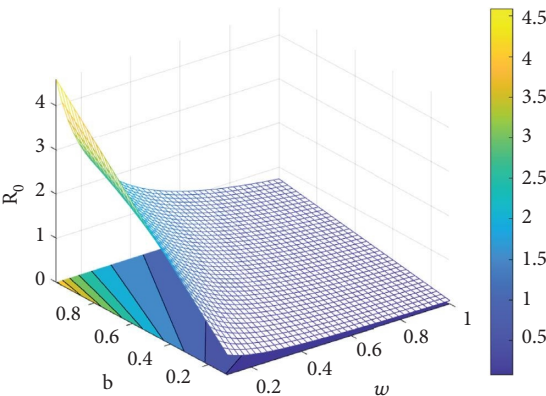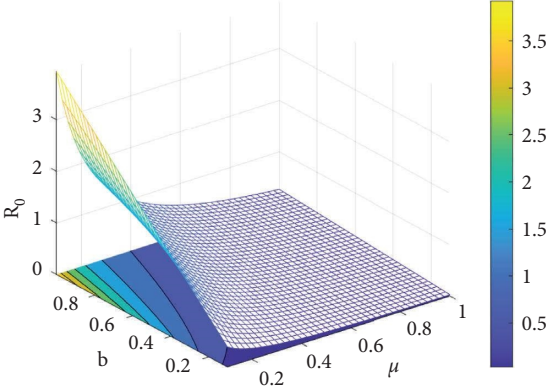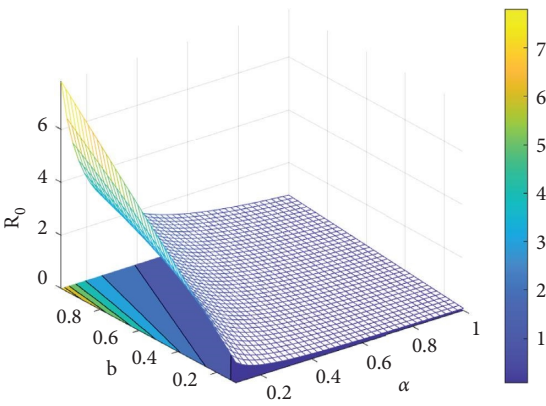

FIGURE 5: The dynamics of sensitivity analysis with respect to parameters μ and b with R_0.

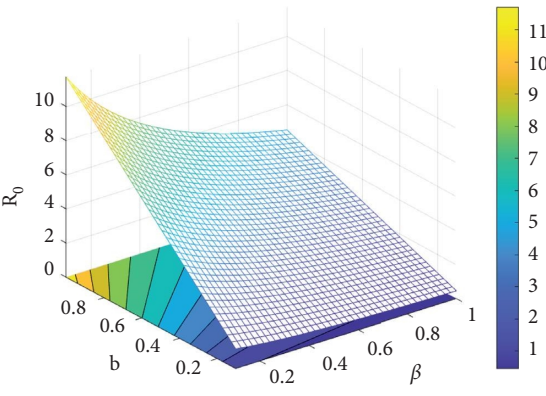FIGURE 3: The dynamics of sensitivity analysis with respect to parameters λ and b with R_0.

FIGURE 6: The dynamics of Sensitivity Analysis with respect to parameters α and b with R_0.

FIGURE 4: The dynamics of sensitivity analysis with respect to parameters ω and b with R_0.

FIGURE 7: The dynamics of sensitivity analysis with respect to parameters β and b with R_0.

TABLE 3: Sensitivity of the R_0 versus proposed parameters.

Parameter	Sensitivity index	Value	Parameter	Sensitivity index	Value
b	$\mathbf{s}_b^{R_0}$	1.0000	ω	$\mathbf{s}_\omega^{R_0}$	0.2188
α	$\mathbf{s}_\alpha^{R_0}$	−0.9979	β	$\mathbf{s}_\beta^{R_0}$	−0.2187
μ	$\mathbf{s}_\mu^{R_0}$	−0.0014	λ	$\mathbf{s}_\lambda^{R_0}$	−0.0007

parameters constant. Furthermore, in Table 3, if the sensitivity index $\mathbf{s}_p^{R_0}$ for parameter p goes negatively, then there is an inverse effect on R_0. The parameters show the negative effect must be minimized for the sake of the spread of infection in the population. Moreover, the sensitivity index of b is positive at its peak.

6. Ulam–Hyers Stability

Stability theory is an important branch of the qualitative theory of differential equations. As we know, the computation of exact solutions to some problems is quite challenging to obtain. Therefore, various numerical techniques were developed to find a solution. In this regard, we check the stability of the given problem. We can find various types of stability in literature, including Lyapunov, exponential, and asymptotic. But the most important type of stability, which is first introduced by Ulam in 1940 is called Ulam stability. He posed a problem about the stability of functional equations. The proper introduction was given by Hyers in 1941. Therefore, this stability was named Ulam–Hyers stability (see [72, 73]). The said stability results have been extended and generalized by researchers for difference and functional equations in different directions. From a numerical and optimization point of view, Ulam–Hyers stability is essential because it provides a bridge between the exact and numerical solutions. The said stability is most useful and also easy to establish for the approximated solution o model (1). Therefore, in this section, by the use of nonlinear functional analysis, some adequate conditions are constructed for the mentioned stability of the proposed model (1).

$$
\left.\begin{aligned}
{}_0^{\mathrm{FFP}}D^{\,\nu,\pi}U(t) &= \Lambda - \frac{bUV}{1+aV} - (\omega-\mu+\alpha)U, \\[6pt]
{}_0^{\mathrm{FFP}}D^{\,\nu,\pi}W(t) &= \frac{bUV}{1+aV} - (\lambda+\mu+\beta)V, \\[6pt]
{}_0^{\mathrm{FFP}}D^{\,\nu,\pi}Q(t) &= \lambda V - (\mu+\xi+\gamma+d)W, \\[6pt]
{}^{\mathrm{FFP}}D^{\,\nu,\pi}X(t) &= \alpha U + \beta V + \alpha W - (\mu+\rho)Q, \\[6pt]
{}^{\mathrm{FFP}}D_0^{\,\nu,\pi}Y(t) &= \omega U + \rho Q + \gamma W - \mu X_\nu, \\[6pt]
&= \xi W + \gamma W - \delta Y.
\end{aligned}\right\}. \tag{35}
$$

We express model (35) as

$$
\left.\begin{aligned}
f_1(t,U,D,W,Q,X,Y) &= \Lambda - \frac{bUV}{1+aV} - (\omega-\mu+\alpha)U, \\[6pt]
f_2(t,U,D,W,Q,X,Y) &= \frac{bUV}{1+aV} - (\lambda+\mu+\beta)V, \\[6pt]
f_3(t,U,D,W,Q,X,Y) &= \lambda V - (\mu+\xi+\gamma+d)W, \\[6pt]
f_4(t,U,D,W,Q,X,Y) &= \alpha U + \beta V + dW - (\mu+\rho)Q, \\[6pt]
f_5(t,U,D,W,Q,X,Y) &= \omega U + \rho Q + \gamma W - \mu X_\nu, \\[6pt]
f_6(t,U,D,W,Q,X,Y) &= \xi W + \gamma W - \delta Y.
\end{aligned}\right\}. \tag{36}
$$

The proposed problem (35) can be reformulated in the following form:

$$
\left.\begin{aligned}
{}_0^{c}D^{\,\pi}U(t) &= \nu t^{\nu-1} f_1(t,U,D,W,Q,X,Y), \\[6pt]
{}_0^{c}D^{\,\pi}V(t) &= \nu t^{\nu-1} f_2(t,U,D,W,Q,X,Y), \\[6pt]
{}_0^{c}D^{\,\pi}V(t) &= \nu t^{\nu-1} f_3(t,U,D,W,Q,X,Y), \\[6pt]
{}_0^{c}D^{\,\pi}V(t) &= \nu t^{\nu-1} f_4(t,U,D,W,Q,X,Y), \\[6pt]
{}_0^{c}D^{\,\pi}V(t) &= \nu t^{\nu-1} f_5(t,U,D,W,Q,X,Y), \\[6pt]
{}_0^{c}D^{\,\pi}V(t) &= \nu t^{\nu-1} f_6(t,U,D,W,Q,X,Y).
\end{aligned}\right\}. \tag{37}
$$

With the help of (36), we can write the considered system (33) as

$$
\begin{aligned}
{}_0^{c}D^{\,\pi}K(t) &= \nu t^{\nu-1}\mathscr{F}(t,K(t)),\ 0<\nu<1,\ 0<\pi<1, \\
K(0) &= K_0.
\end{aligned} \tag{38}
$$

On applying the integral, we get the solution of (38) as

$$
K(t) = K_0(t) + \frac{\nu}{\Gamma(\pi)}\int_0^t x^{\nu-1}(t-x)^{\pi-1}\mathscr{F}(x,K(x))\mathrm{d}x, \tag{39}
$$

where

$$K(t) = \begin{cases} U(t) \\ V(t) \\ W(t) \\ Q(t) \\ X(t) \\ Y(t) \end{cases}, K_0(t) = \begin{cases} U_0 \\ V_0 \\ W_0 \\ Q_0 \\ X_0 \\ Y_0 \end{cases}, \tag{40}$$

$$\mathscr{F}(t, K(t)) = \begin{cases} f_1(t, U, D, W, Q, X, Y), \\ f_2(t, U, D, W, Q, X, Y), \\ f_3(t, U, D, W, Q, X, Y), \\ f_4(t, U, D, W, Q, X, Y), \\ f_5(t, U, D, W, Q, X, Y), \\ f_6(t, U, D, W, Q, X, Y). \end{cases}$$

For Ulam–Hyers stability, let $\wp \in C(\mathfrak{F})$, which is a small perturbation independent of solution. In addition, $|\wp(t)| \le \varepsilon$, for $\varepsilon > 0$; $_0^{\text{FFP}}D^{\nu,\pi}K(t) = \mathscr{F}(t, K(t)) + \wp(t)$.

Lemma 3. *The solution of the perturbed problem,*

$$_0^c D^\pi K(t) = \nu t^{\nu-1} \mathscr{F}(t, K(t)) + \wp(t), \tag{41}$$
$$K(0) = K_0,$$

satisfies the following relation

$$\left| K(t) - \left(K_0(t) + \frac{\nu}{\Gamma(\pi)} \int_0^t x^{\nu-1}(t-x)^{\pi-1} \mathscr{F}(x, K(x)) \mathrm{d}x \right) \right| \le \Delta\varepsilon. \tag{42}$$

Proof 4. According to (37), the solution of (39) is given by

$$K(t) = K_0(t) + \frac{\nu}{\Gamma(\pi)} \int_0^t x^{\nu-1}(t-x)^{\pi-1}[\mathscr{F}(x, K(x))x + \wp(t)]\mathrm{d}x. \tag{43}$$

Using $|\wp(t)| \le \varepsilon$ in (43), one can easily get the relation (41). □

Theorem 5. *In view of the inequality (42), and hypothesis given in (44), if the condition $\Delta\mathfrak{L}_{\mathscr{F}} < 1$ holds, then the solution of problem (33) is Ulam–Hyers stable, where*

$$|\mathscr{F}(x, K) - \mathscr{F}(x, \overline{K})| \le \mathfrak{Q}_{\mathscr{F}}|K - \overline{K}|, \mathfrak{L}_{\mathscr{F}} > 0. \tag{44}$$

Proof 5. Suppose $\mathscr{W}$ is a unique solution and K be any other solution of (37) in Banach space $\mathfrak{B}$; then,

$$\begin{aligned} |K(t) - \mathscr{W}(t)| &= \left| K(t) - \left(\mathscr{W}_0(t) + \frac{\nu}{\Gamma(\pi)} \int_0^t x^{\nu-1}(t-x)^{\pi-1} \mathscr{F}(x, \mathscr{W}(x)) \mathrm{d}x \right) \right|, \\ &\le \left| K(t) - \left(K_0(t) + \frac{\nu}{\Gamma(\pi)} \int_0^t x^{\nu-1}(t-x)^{\pi-1} \mathscr{F}(x, K(x)) \mathrm{d}x \right) \right| \\ &+ \left| \left(K_0(t) + \frac{\nu}{\Gamma(\pi)} \int_0^t x^{\nu-1}(t-x)^{\pi-1} \mathscr{F}(x, K(x)) \mathrm{d}x \right) \right. \\ &- \left(\mathscr{W}_0(t) + \frac{\nu}{\Gamma(\pi)} \int_0^t x^{\nu-1}(t-x)^{\pi-1} \mathscr{F}(x, \mathscr{W}(x)) \mathrm{d}x \right) \\ &\le \Delta\varepsilon + \mathfrak{L}_{\mathscr{F}}\|K - \mathscr{W}\|. \end{aligned} \tag{45}$$

From (45), we can write

$$\|K - \mathscr{W}\| \le \mathfrak{U}_{\nu,\pi}\varepsilon, \tag{46}$$

where $\mathfrak{A} > 0, \forall K \in \mathfrak{B}$. Thus, from the result (43), we conclude that (33) is Ulam–Hyers stable. □
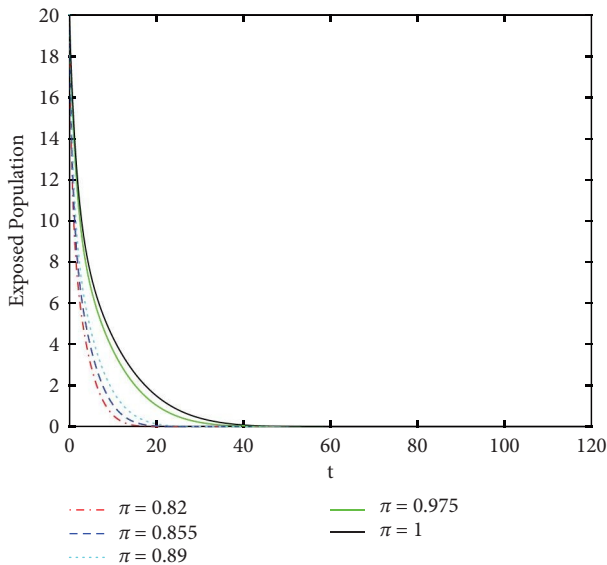
7. Numerical Scheme

Nonlinear problems are more difficult than linear ones to solve analytically. Therefore, researchers have implemented efficient and accurate numerical schemes for the treatment of nonlinear problems to explore the dynamics of real-world

problems more precisely. To tackle this nonlinear problem, from definition (3), we use the Adams–Bashforth scheme for the justification of our work.

$$
U(l+1) = U(0) + \frac{v\hbar^\pi}{\Gamma(\pi+2)} \sum_{j=0}^{f} \left[t_{(j)}^{v-1} u\left(U_{(j)}, t_j\right) \right.
$$

$$
\times \left((f+1-j)^v (f-j+2+v) - (f-j)^v (f-j+2+2v) \right)
$$

$$
\left. - t_{(j-1)}^{v-1} v\left(U_{(j-1)}, t_{(j-1)}\right) \left((f+1-j)^v + 1 - (f-j)^v (f-j+1+v) \right) \right),
$$

$$
V(l+1) = V(0) + \frac{v\hbar^\pi}{\Gamma(\pi+2)} \sum_{j=0}^{f} \left[t_{(j)}^{v-1} u\left(V_{(j)}, t_j\right) \right.
$$

$$
\times \left((f+1-j)^v (f-j+2+v) - (f-j)^v (f-j+2+2v) \right)
$$

$$
\left. - t_{(j-1)}^{v-1} v\left(V_{(j-1)}, t_{(j-1)}\right) \left((f+1-j)^v + 1 - (f-j)^v (f-j+1+v) \right) \right),
$$

$$
W(l+1) = W(0) + \frac{v\hbar^\pi}{\Gamma(\pi+2)} \sum_{j=0}^{f} \left[t_{(j)}^{v-1} u\left(W_{(j)}, t_j\right) \right.
$$

$$
\times \left((f+1-j)^v (f-j+2+v) - (f-j)^v (f-j+2+2v) \right)
$$

$$
\left. - t_{(j-1)}^{v-1} v\left(W_{(j-1)}, t_{(j-1)}\right) \left((f+1-j)^v + 1 - (f-j)^v (f-j+1+v) \right) \right),
$$

$$
Q(l+1) = Q(0) + \frac{v\hbar^\pi}{\Gamma(\pi+2)} \sum_{j=0}^{f} \left[t_{(j)}^{v-1} u\left(Q_{(j)}, t_j\right) \right.
$$

$$
\times \left((f+1-j)^v (f-j+2+v) - (f-j)^v (f-j+2+2v) \right)
$$

$$
\left. - t_{(j-1)}^{v-1} v\left(Q_{(j-1)}, t_{(j-1)}\right) \left((f+1-j)^v + 1 - (f-j)^v (f-j+1+v) \right) \right),
$$

$$
X_v(l+1) = X_v(0) + \frac{v\hbar^\pi}{\Gamma(\pi+2)} \sum_{j=0}^{f} \left[t_{(j)}^{v-1} u\left(X_{v\,(j)}, t_j\right) \right.
$$

$$
\times \left((f+1-j)^v (f-j+2+v) - (f-j)^v (f-j+2+2v) \right)
$$

$$
\left. - t_{(j-1)}^{v-1} v\left(X_{v(j-1)}, t_{(j-1)}\right) \left((f+1-j)^v + 1 - (f-j)^v (f-j+1+v) \right) \right),
$$

$$
Y(l+1) = Y(0) + \frac{v\hbar^\pi}{\Gamma(\pi+2)} \sum_{j=0}^{f} \left[t_{(j)}^{v-1} u\left(Y_{(j)}, t_j\right) \right.
$$

$$
\times \left((f+1-j)^v (f-j+2+v) - (f-j)^v (f-j+2+2v) \right)
$$

$$
\left. - t_{(j-1)}^{v-1} v\left(Y_{(j-1)}, t_{(j-1)}\right) \left((f+1-j)^v + 1 - (f-j)^v (f-j+1+v) \right) \right).
$$

$$(47)$$

TABLE 4: Table for numerical values of parameters.

Symbol	Description of parameter	Dimension	Value
Λ	Recruitment rate [49]	Month^{-1}	$10000/50 \times 365$
μ	Natural death rate. [49]	Month^{-1}	$1/50 \times 365$
b	Transmission rate	Month^{-1}	0.00019
a	Psychological effect on human, [55]	Month^{-1}	0.0701
ξ	Recovery rate of infected population, [48]	Month^{-1}	0.01
α	Period of quarantine in susceptible population.	Month^{-1}	0.0701
β	Period of quarantine in exposed population	Month^{-1}	0.13
d	Period of quarantine in infected population	Month^{-1}	0.0701
ω	Vaccination rate of susceptible population	Month^{-1}	0.0001
γ	Vaccination rate of infected population	Month^{-1}	0.00001
ρ	Vaccination rate of quarantine population	Month^{-1}	0.0002
δ	Death rate of recovered population	Month^{-1}	0.002
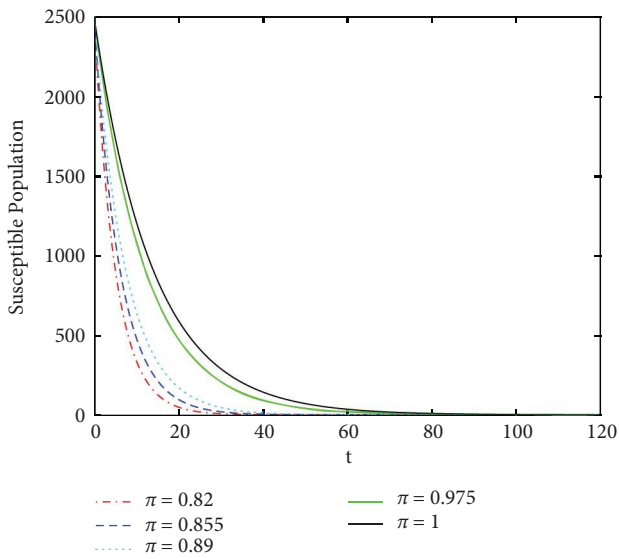
FIGURE 8: The dynamics of susceptible human population for various fractional orders π and for fractal order $v = 0.5$.

FIGURE 9: The dynamics of exposed human population for various fractional orders v and for fractal order $\pi = 0.5$.
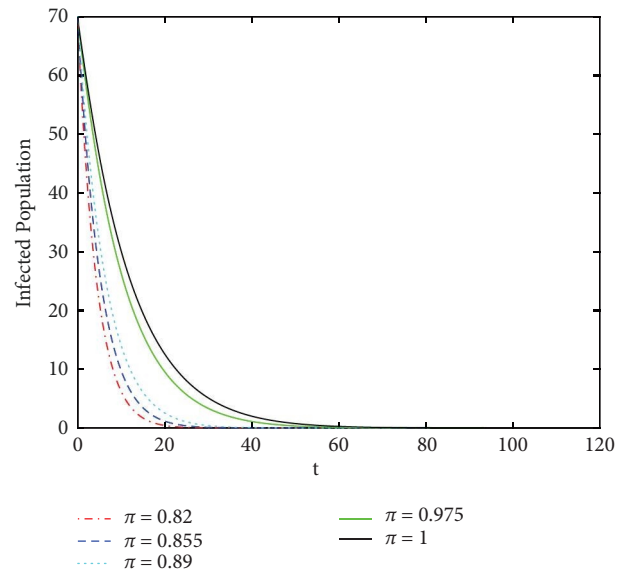
FIGURE 10: The dynamics of infected human population for various fractional orders v and for fractal order $\pi = 0.5$.
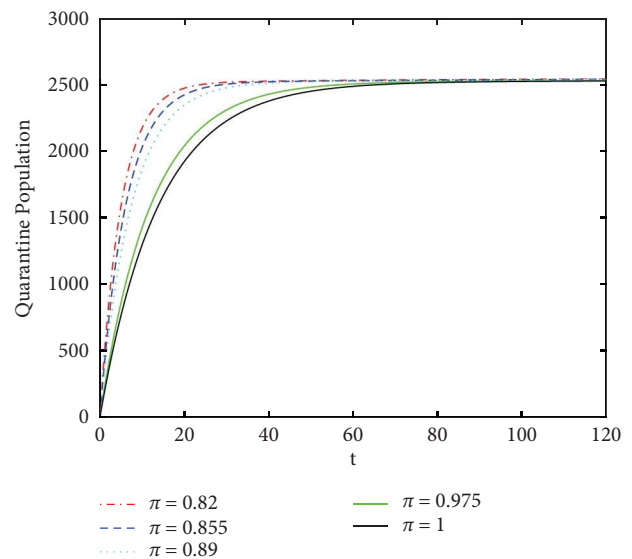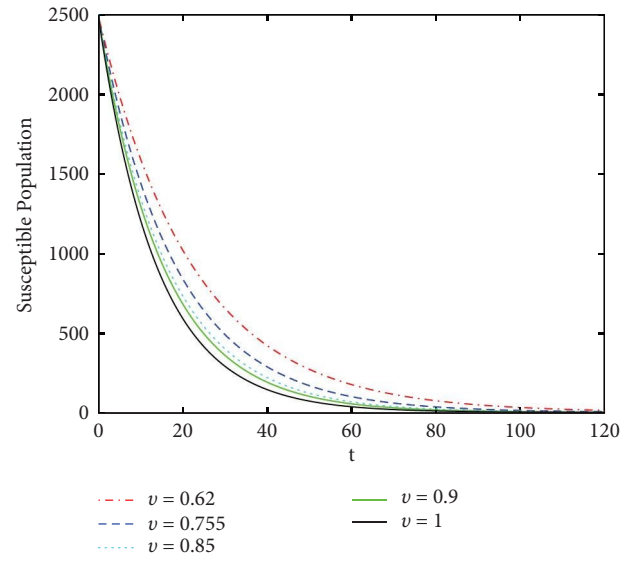

FIGURE 11: The dynamics of quarantine human population for various fractional orders v and for fractal order $\pi = 0.5$.
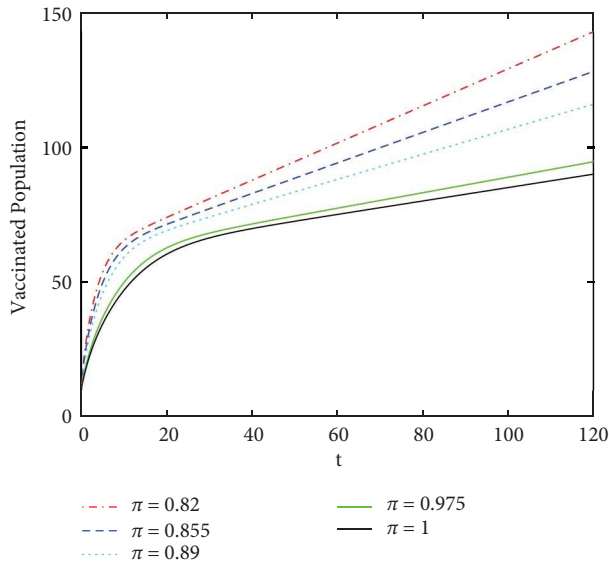
Figure 12: The dynamics of vaccinated human population for various fractional orders v and for fractal order $\pi = 0.5$.

Figure 14: The dynamics of susceptible human population for various fractal orders π and for fractional order $v = 0.5$.
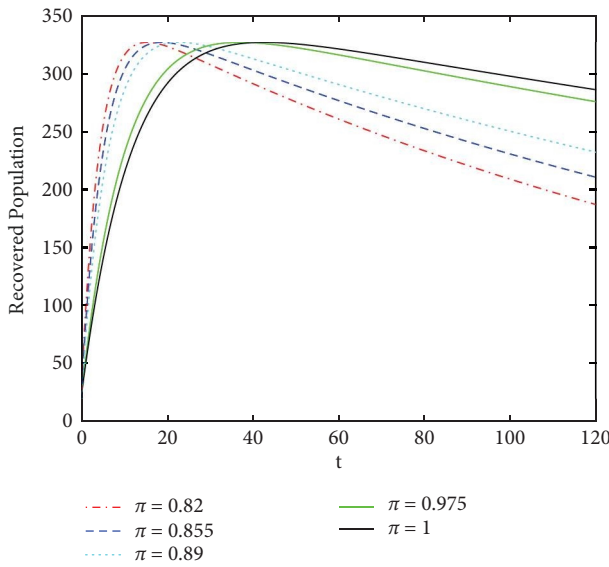

Figure 13: The dynamics of recovered human population for various fractional orders v and for fractal order $\pi = 0.5$.
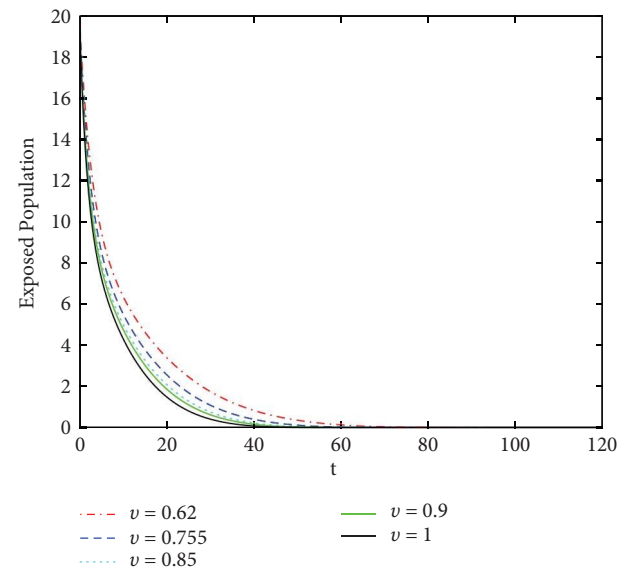

Figure 15: The dynamics of exposed human population for various fractal orders π and for fractional order $v = 0.5$.

Remark 1. Here it should be kept in mind that the Adams–Bashforth method preserves the basic type of numerical stability associated with the usual one-step numerical methods including Euler, backward Euler, and trapezoidal. Furthermore, it is a $(l + 1)$-step explicit method, and whose truncation error is of size $O(h^{l+2})$. For detailed convergence and stability of the Adams–Bashforth method, we refer for the readers to see [74].

8. Numerical Results and Discussion

To simulate our model, we use the numerical values given in Table 4.

In this section, we explain the dynamics of the proposed model from graphical results such that the bar chart (2) shows the quantity of sensitivity index of parameters associated with R_0, in which two parameters b and α have a
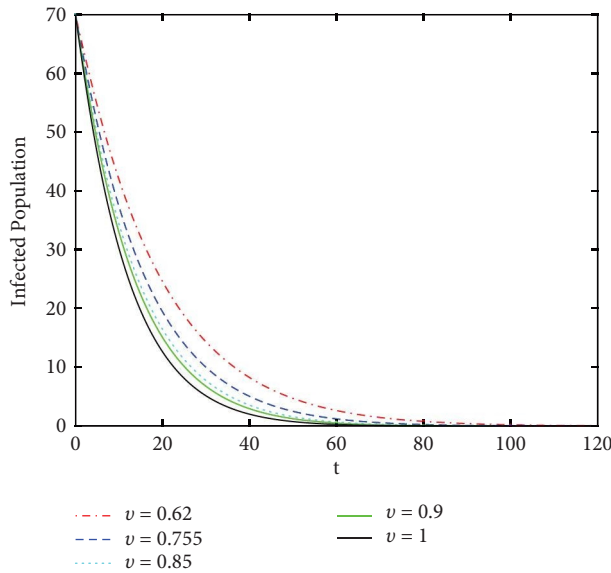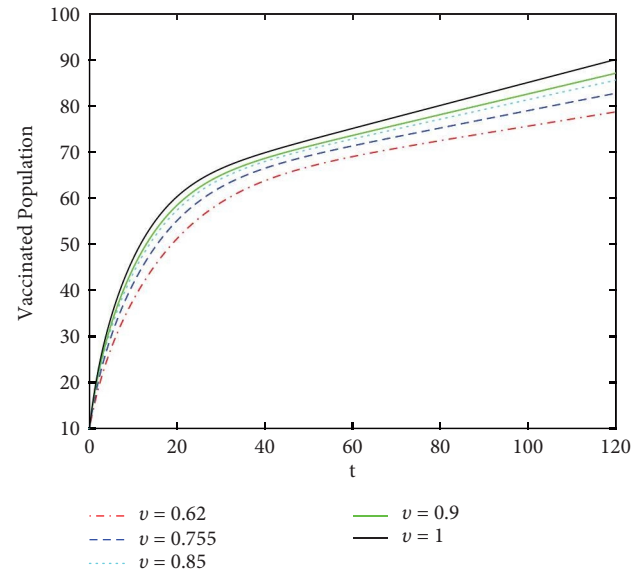
FIGURE 16: The dynamics of infected human population for various fractal orders π and for fractional order $v = 0.5$.

FIGURE 18: The dynamics of vaccinated human population for various fractal orders π and for fractional order $v = 0.5$.
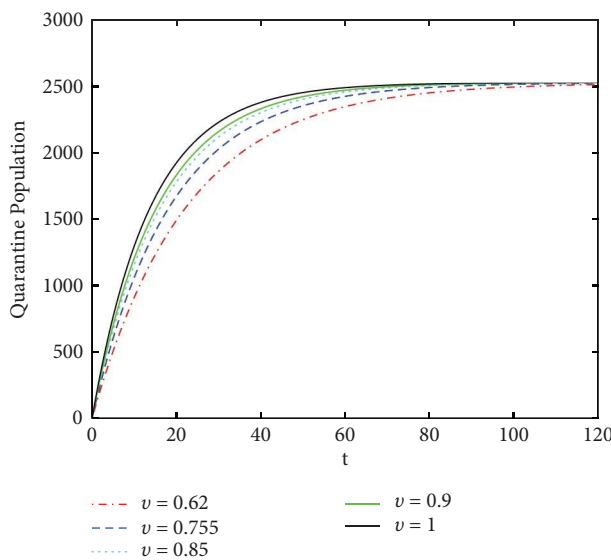

FIGURE 17: The dynamics of quarantine human population for various fractal orders π and for fractional order $v = 0.5$.
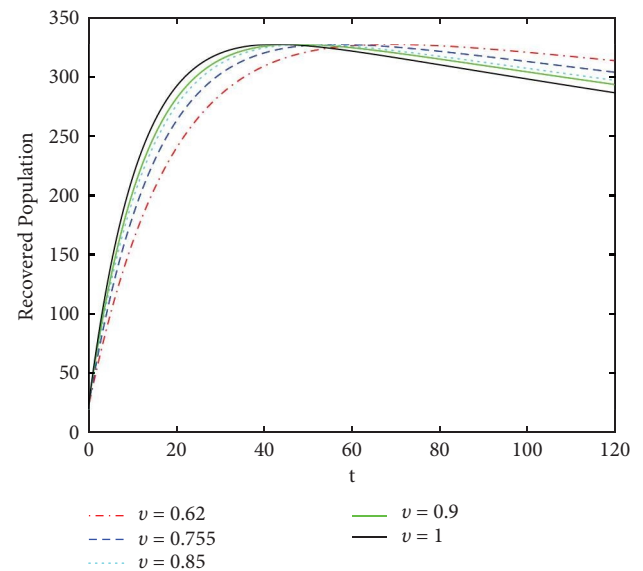

FIGURE 19: The dynamics of recovered human population for various fractal orders π and for fractional order $v = 0.5$.

large effect on R_0. From Figures 3–7, we see the dynamics of R_0 by using numerical values of parameters λ, ω, μ, α, and β. Furthermore, Figures 8–13 show the stable behavior of susceptible, exposed, infected, quarantine, vaccinated, and recovered population, respectively, with a variation in fractal order π and using value of fractional order $v = 0.5$. Moreover, Figures 14–19 show the behavior of the model with each compartment under different fractional order and using value of fractal order $\pi = 0.5$. While in Figures 20, 21, 22, 23, 24, and 25, we plot the solution for different fractal-fractional order. Here, we compared the real available reported cases of infection in Pakistan for 200 days from 15th March 2021 to 30th September 2021. The details about the COVID-19 situation in Pakistan can be found in [75, 76], and [77]. Also, some real data in comparison with fractional order simulation has been plotted in [78] recently. We see
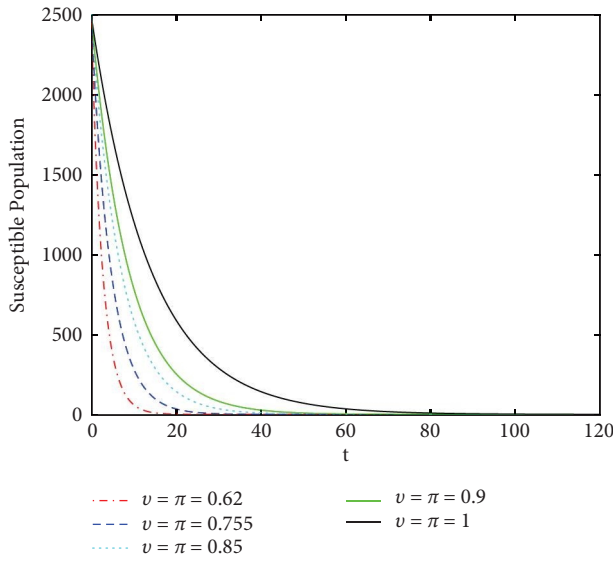
Figure 20: The dynamics of susceptible human population for various fractal-fractional orders.
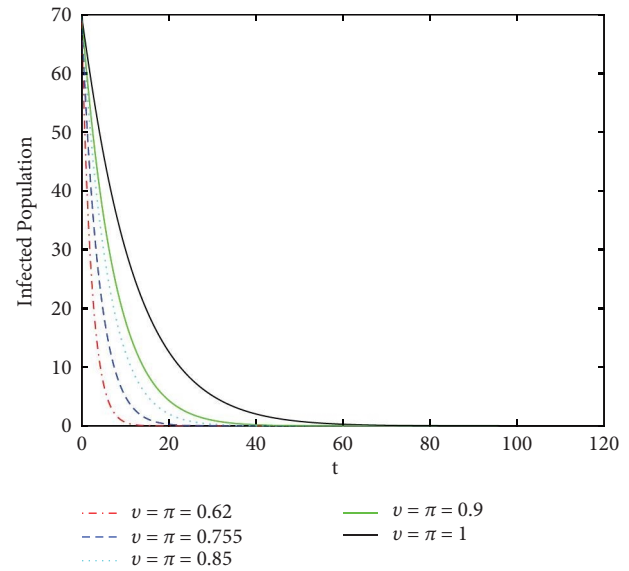

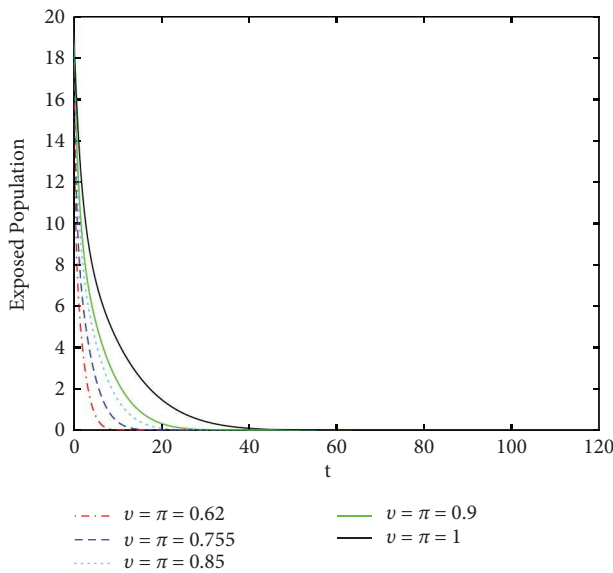Figure 22: The dynamics of infected human population for various fractal-fractional orders.

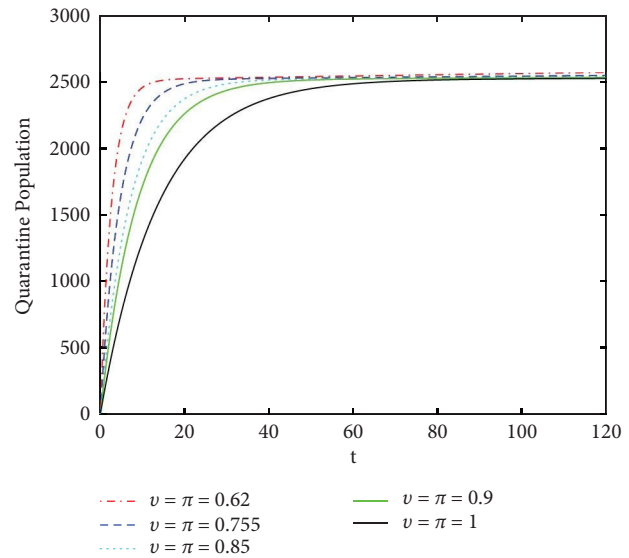Figure 21: The dynamics of exposed human population for various fractal-fractional orders.

Figure 23: The dynamics of quarantine human population for various fractal-fractional orders.

that the numerical simulation at two different fractional orders coincides very well with the plot of real data as shown in Figure 26. The graphical results also reveal that when the

fractal v and fractional π orders approach 1, then model 1 is reduced to the classical order model.

From Figure 26, it is clear that the real data plot and the simulated data graph are closely related. Moreover,
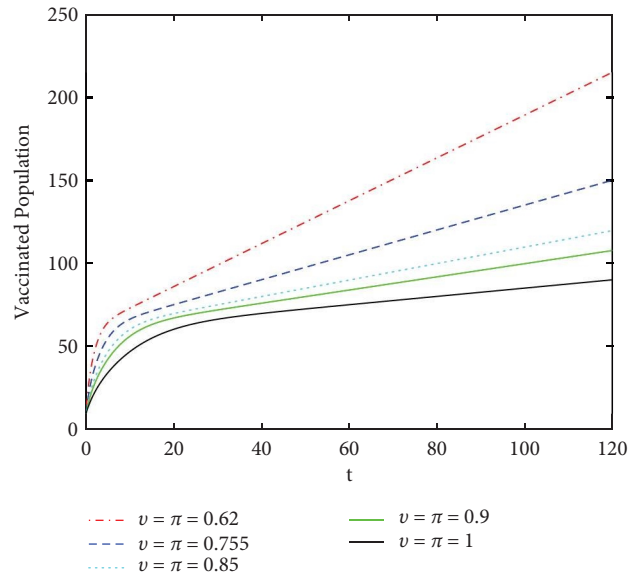
FIGURE 24: The dynamics of vaccinated human population for various fractal-fractional orders.
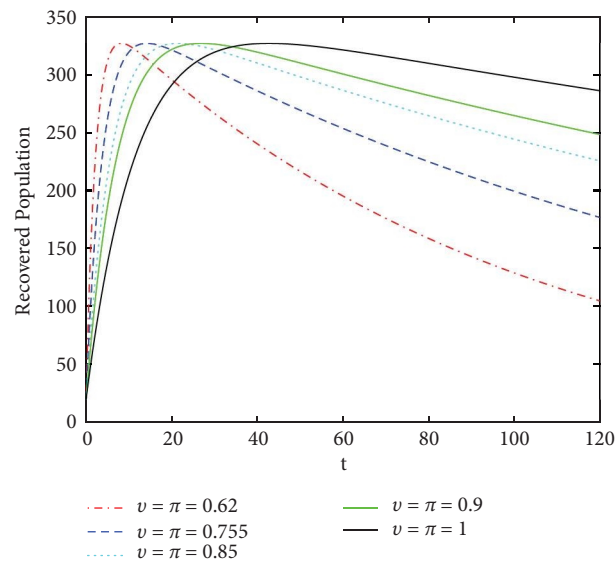

FIGURE 25: The dynamics of recovered human population for various fractal-fractional orders.

by fitting the real data, we can obtain the numerical values of the parameters of model 1 given in Table 4. Moreover, the model is numerically stable and takes less time and memory during simulation using the Adams–Bashforth scheme due to the nonlinearity and complexity of the problem.
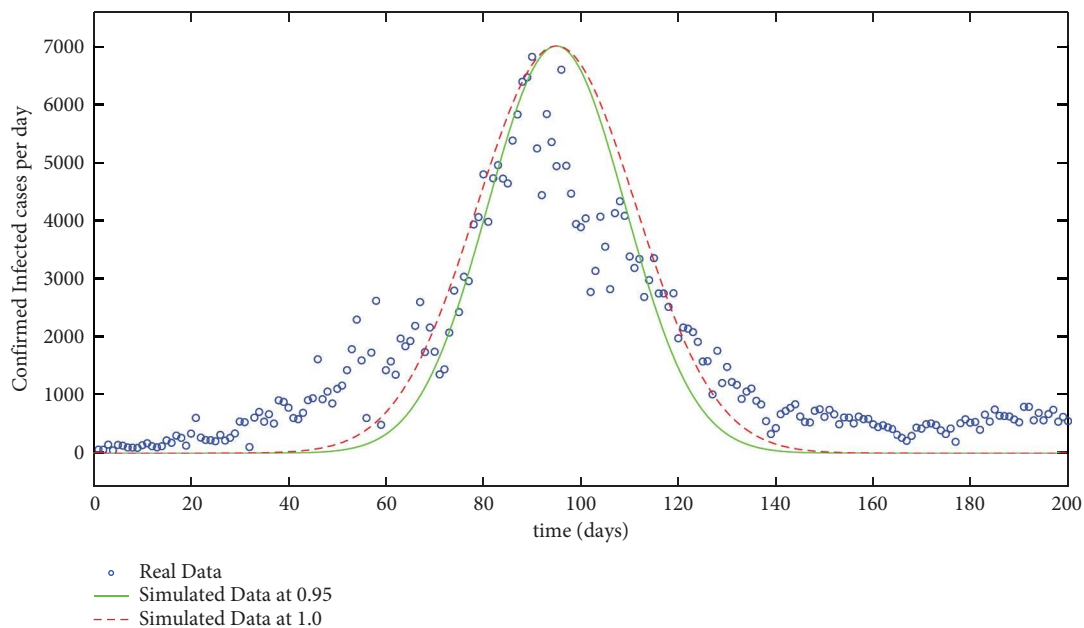
FIGURE 26: Comparison between real reported infected cases with simulated data at two different fractional orders.

9. Conclusion

We have studied the compartmental model of COVID-19 which has been consisting of susceptible, infected, quarantined, vaccinated, and recovered human populations. The model has been specifically proposed for the implementation of a vaccinated class. The fractal-fractional calculus has been used to understand the dynamics of fractal order π and fractional order v. We have also investigated some results devoted to local and global stability for the proposed model based on the Jacobian matrix and the Lyapunov function method. Both local and global type stabilities have been demonstrated under the disease-free and endemic equilibrium points by showing that $R_0 < 1$ and $R_0 > 1$, respectively. For the sensitivity analysis of each parameter, we have investigated global sensitivity analysis to justify the said feature. Furthermore, some results necessary for numerical stability based on the Ulam–Hyers concept have also been studied. Numerical simulations have been presented by means of the Adams–Bashforth scheme. Some discussion about the convergence and numerical stability of the proposed method has been given in Remark 1. Numerical results have been displayed in different fractional orders graphically to understand the dynamics of the model. We have given a comparison between real reported and simulated data in the case of the infected class. Both curves are closely agreed which shows the efficiency of the proposed numerical method. The given detail can be extended to more complex dynamical systems in the future.

Data Availability

All the data used in the paper are included in the manuscript.

Conflicts of Interest

The authors declare that they have no conflicts of interest regarding this work.

Authors' Contributions

All authors have contributed equally.

Acknowledgments

References

[1] World Health Organization (WHO), "Naming the coronavirus disease (COVID-19) and the virus that causes it, Archived from the original on 28 February 2020," 2020, https://www.who.int/emergencies/diseases/novel-cor.

[2] Million-Excess-Deaths-Were-Associated, "Million-excess-deaths-were-associated," 2022, https://www.who.int/news/item/05-05-2022-14.9-million-excess-deaths-were-associated-with-the-covid-19-pandemic-in-2020-and-2021.

[3] S. Zhao, S. S. Musa, Q. Lin et al., "Estimating the unreported number of novel coronavirus (2019-nCoV) cases in China in the first half of January 2020, a data-driven Modelling analysis of the early outbreak," Journal of Clinical Medicine, vol. 9, no. 2, p. 388, 2020.

[4] I. Nesteruk, "Statistics based predictions of coronavirus 2019-nCoV spreading in mainland China," medRxiv, vol. 4, no. 1, pp. 1988-1989, 2020.

[5] D. S. I. Hui, E. I Azhar, T. A. Madani et al., "The continuing 2019-nCoV epidemic threat of novel coronaviruses to global

health-The latest 2019 novel coronavirus outbreak in Wuhan, China," *International Journal of Infectious Diseases*, vol. 91, no. 6, pp. 264–266, 2020.

[6] S. Zhao, Q. Lin, J. Ran et al., "Preliminary estimation of the basic reproduction number of novel coronavirus (2019-nCoV) in China, from 2019 to 2020: a data-driven analysis in the early phase of the outbreak," *International Journal of Infectious Diseases*, vol. 92, pp. 214–217, 2020.

[7] K. Shah, R. U. Din, W. Deebani, P. Kumam, and Z. Shah, "On nonlinear classical and fractional order dynamical system addressing COVID-19," *Results in Physics*, vol. 24, Article ID 104069, 2021.

[8] F. Mainardi, "An historical perspective on fractional calculus in linear viscoelasticity," *Fractional Calculus and Applied Analysis*, vol. 15, no. 4, pp. 712–717, 2012.

[9] N. S. Goel, S. C. Maitra, and E. W. Montroll, "On the Volterra and other nonlinear models of interacting populations," *Reviews of Modern Physics*, vol. 43, no. 2, pp. p231–276, 1971.

[10] P. Zhou, X. L. Yang, X. G. Wang et al., "A pneumonia outbreak associated with a new coronavirus of probable bat origin," *Nature*, vol. 579, no. 7798, pp. 270–273, 2020.

[11] Q. Li, X. Guan, P. Wu et al., "Early transmission dynamics in Wuhan, China, of novel coronavirus infected pneumonia," *New England Journal of Medicine*, vol. 382, no. 13, pp. 1199–1207, 2020.

[12] I. I. Bogoch, A. Watts, A. Thomas-Bachli, C. Huber, M. U. G. Kraemer, and K. Khan, "Pneumonia of unknown aetiology in Wuhan, China: potential for international spread via commercial air travel," *Journal of Travel Medicine*, vol. 27, no. 2, Article ID taaa008, 2020.

[13] A. B. Gumel, S. Ruan, T. Day et al., "Modelling strategies for controlling SARS out breaks," *Proceedings of the Royal Society of London B*, vol. 271, no. 1554, pp. 2223–2232, 2004.

[14] A. Atangana and S. İğret Araz, "Modeling third waves of Covid-19 spread with piecewise differential and integral operators: Turkey, Spain and Czechia," *Results in Physics*, vol. 29, Article ID 104694, 2021.

[15] A. Atangana, "Modelling the spread of COVID-19 with new fractal-fractional operators: can the lockdown save mankind before vaccination?" *Chaos, Solitons & Fractals*, vol. 136, Article ID 109860, 2020.

[16] A. Atangana and S. İğret Araz, "Mathematical model of COVID-19 spread in Turkey and South Africa: theory, methods, and applications," *Advances in Difference Equations*, vol. 2020, no. 1, pp. 659–689, 2020.

[17] R. Prieto Curiel and H. González Ramírez, "Vaccination strategies against COVID-19 and the diffusion of anti- vaccination views," *Scientific Reports*, vol. 11, no. 1, p. 6626, 2021.

[18] C. A. B. Pearson, F. Bozzani, and S. R. Procter, *Health Impact and Cost-Effectiveness of COVID-19 Vaccination in Sindh Province Pakistan*, medRxiv, Spring Harbor, NY, USA, 2021.

[19] J. T. Wu, K. Leung, and G. M. Leung, "Nowcasting and forecasting the potential domestic and international spread of the 2019-nCoV outbreak originating in Wuhan, China: a modelling study," *The Lancet*, vol. 395, no. 10225, pp. 689–697, 2020.

[20] M. S. Arshad, D. Baleanu, M. B. Riaz, and M. Abbas, "A novel 2-stage fractional Runge-Kutta method for a TimeFractional logistic growth model," *Discrete Dynamics in Nature and Society*, vol. 2020, Article ID 1020472, 8 pages, 2020.

[21] T. Abdeljawad, Q. M. Al-Mdallal, and F. Jarad, "Fractional logistic models in the frame of fractional operators generated by conformable derivatives, Chaos," *Solitons & Fractals*, vol. 119, pp. 94–101, 2019.

[22] F. Liu and K. Burrage, "Novel techniques in parameter estimation for fractional dynamical models arising from biological systems," *Computers & Mathematics with Applications*, vol. 62, no. 3, pp. 822–833, 2011.

[23] M. T. Hoang and O. F. Egbelowo, "Dynamics of a fractional-order hepatitis b epidemic model and its solutions by nonstandard numerical schemes," *Mathematical Modelling and Analysis of Infectious Diseases*, vol. 2020, pp. 127–153, 2020.

[24] M. A. Khan and A. Atangana, "Modeling the dynamics of novel coronavirus (2019-nCov) with fractional derivative," *Alexandria Engineering Journal*, vol. 59, no. 4, pp. 2379–2389, 2020.

[25] M. A. Khan, A. Atangana, E. Alzahrani, and Fatmawati, "The dynamics of COVID-19 with quarantine and isolation," *Advances in Difference Equations*, vol. 2020, no. 1, pp. 425–522, 2020.

[26] S. Boccaletti, W. Ditto, G. Mindlin, and A. Atangana, "Modeling and forecasting of epidemic spreading: the case of Covid-19 and beyond," *Chaos, Solitons & Fractals*, vol. 135, Article ID 109794, 2020.

[27] E. Atangana and A. Atangana, "Facemasks simple but powerful weapons to protect against COVID-19 spread: can they have sides effects?" *Results in Physics*, vol. 19, Article ID 103425, 2020.

[28] S. T. Thabet, M. S. Abdo, K. Shah, and T. Abdeljawad, "Study of transmission dynamics of COVID-19 mathematical model under ABC fractional order derivative," *Results in Physics*, vol. 19, Article ID 103507, 2020.

[29] J. T. Machado, V. Kiryakova, and F. Mainardi, "Recent history of fractional calculus," *Communications in Nonlinear Science and Numerical Simulation*, vol. 16, no. 3, pp. 1140–1153, 2011.

[30] F. C. Meral, T. J. Royston, and R. Magin, "Fractional calculus in viscoelasticity: an experimental study," *Communications in Nonlinear Science and Numerical Simulation*, vol. 15, no. 4, pp. 939–945, 2010.

[31] R. L. Magin, "Fractional calculus in bioengineering, part 1," *Critical Reviews in Biomedical Engineering*, vol. 32, no. 1, pp. 1–104, 2004.

[32] M. Dalir and M. Bashour, "Applications of fractional calculus," *Applied Mathematical Sciences*, vol. 4, no. 21, pp. 1021–1032, 2010.

[33] L. M. Richard, *Fractional Calculus in Bioengineering*, Begell House, Danbury, Connecticut, 2006.

[34] A. Y. Rossikhin and M. V. Shitikova, "Applications of Fractional Calculus to Dynamic Problems of Linear and Nonlinear Hereditary Mechanics of Solids," *Appl. Mech. Rev*, vol. 50, pp. 15–67, 1997.

[35] F. Mainardi, "Fractional calculus," in *Fractals and Fractional Calculus in Continuum Mechanics*Springer, Berlin, Germany, 1997.

[36] B. B. Mandelbrot, "How long is the coast of Britain? Statistical self-similarity and fractional dimension," *Science*, vol. 156, no. 3775, pp. 636–638, 1967.

[37] B. B. Mandelbrot, D. E. Passoja, and A. J. Paullay, "Fractal character of fracture surfaces of metals," *Nature*, vol. 308, no. 5961, pp. 721-722, 1984.

[38] P. R. Massopust, "Fractal surfaces," *Journal of Mathematical Analysis and Applications*, vol. 151, no. 1, pp. 275–290, 1990.

[39] Q. W. Ran and X. Y. Tan, *Wavelet Analysis, Fractional Fourier Transformation and Application*, National Defence Industry Press, Beijing, China, 2002.

[40] M. F. Barnsley, *Fractals Everywhere*, Elsevier, Singapore, 2009.

[41] Z. Sha and H. J. Ruan, *Fractals and Fitting*, Zhen jiang University Press, Hangzhou, China, 2005.

[42] I. Ahmed, I. A. Baba, A. Yusuf, P. Kumam, and W. Kumam, "Analysis of Caputo fractional-order model for COVID-19 with lockdown," *Advances in Difference Equations*, vol. 2020, no. 1, pp. 394–414, 2020.

[43] R. B. Vinter, J. Baillieul, and T. Samad, *Optimal Control and Pontryagin's Maximum Principle, Encyclopedia of Systems and Control*, pp. 950–956, Springer, Berlin, Germany, 2015.

[44] M. J. Mardanov and Y. A. Sharifov, "Pontryagin's maximum principle for the optimal control problems with multipoint boundary conditions," *Abstract and Applied Analysis*, vol. 2015, Article ID 428042, 6 pages, 2015.

[45] L. Zhang, M. U. Rahman, Q. Haidong, and M. Arfan, "Fractal-fractional anthroponotic cutaneous leishmania model study in sense of Caputo derivative," *Alexandria Engineering Journal*, vol. 61, no. 6, pp. 4423–4433, 2022.

[46] R. M. Anderson and R. M. May, *Infectious Diseases of Humans: Dynamics and Control*, Oxford University Press, Oxford, UK, 1992.

[47] P. K. Anderson, A. A. Cunningham, N. G. Patel, F. J. Morales, P. R. Epstein, and P. Daszak, "Emerging infectious diseases of plants: pathogen pollution, climate change and agro-technology drivers," *Trends in Ecology & Evolution*, vol. 19, no. 10, pp. 535–544, 2004.

[48] Y. Gu, M. A. Khan, Y. S. Hamed, and B. F. Felemban, "A comprehensive mathematical model for SARS-CoV-2 in Caputo derivative," *Fractal and Fractional*, vol. 5, no. 4, p. 271, 2021.

[49] Z. H. Shen, Y. M. Chu, M. A. Khan, S. Muhammad, O. A. Al-Hartomy, and M. Higazy, "Mathematical modeling and optimal control of the COVID-19 dynamics," *Results in Physics*, vol. 31, Article ID 105028, 2021.

[50] N. H. J. M. Chitnis, J. M. Hyman, and J. M. Cushing, "Determining important parameters in the spread of malaria through the sensitivity analysis of a mathematical model," *Bulletin of Mathematical Biology*, vol. 70, no. 5, pp. 1272–1296, 2008.

[51] C. Castillo-Chavez and B. Song, "Dynamical models of tuberculosis and their applications," *Mathematical Biosciences and Engineering*, vol. 1, no. 2, pp. 361–404, 2004.

[52] L. S. Pontryagin, *Mathematical Theory of Optimal Processes*, CRC Press, Boca Raton, FA, USA, 1987.

[53] M. Martcheva, *An Introduction to Mathematical Epidemiology*, vol. 61, pp. 9–31, Springer, Berlin, Germany, 2015.

[54] W. H. Fleming and R. W. Rishel, *Deterministic and Stochastic Optimal Control*, Springer Science & Business Media, Berlin, Germany, 2012.

[55] S. Liu, L. Pang, S. Ruan, and X. Zhang, "Global dynamics of avian influenza epidemic models with psychological effect," *Computational and Mathematical Methods in Medicine*, vol. 2015, Article ID 913726, 12 pages, 2015.

[56] F. Bozdag, "The psychological effects of staying home due to the COVID-19 pandemic," *The Journal of General Psychology*, vol. 148, no. 3, pp. 226–248, 2021.

[57] N. H. Sweilam, S. M. Al-Mekhlafi, and A. Almutairi, "Fractal fractional optimal control for a novel malaria mathematical model; a numerical approach," *Results in Physics*, vol. 19, Article ID 103446, 2020.

[58] N. H. Sweilam, S. M. Al-Mekhlafi, and D. G. Mohamed, "Novel chaotic systems with fractional differential operators: numerical approaches," *Chaos, Solitons & Fractals*, vol. 142, Article ID 110475, 2021.

[59] A. Malik, M. Alkholief, F. M. Aldakheel et al., "Sensitivity analysis of COVID-19 with quarantine and vaccination: a fractal-fractional model," *Alexandria Engineering Journal*, vol. 61, no. 11, pp. 8859–8874, 2022.

[60] M. Sinan, K. Shah, P. Kumam et al., "Fractional order mathematical modeling of typhoid fever disease," *Results in Physics*, vol. 32, Article ID 105044, 2022.

[61] A. Atangana, "Fractal-fractional differentiation and integration: c," *Chaos, Solitons & Fractals*, vol. 102, pp. 396–406, 2017.

[62] B. Buonomo and D. Lacitignola, "On the backward bifurcation of a vaccination model with nonlinear incidence," *Nonlinear Analysis Modelling and Control*, vol. 16, no. 1, pp. 30–46, 2011.

[63] H. Lu, Y. Ding, S. Gong, and S. Wang, "Mathematical modeling and dynamic analysis of SIQR model with delay for pandemic COVID-19," *Mathematical Biosciences and Engineering*, vol. 18, no. 4, pp. 3197–3214, 2021.

[64] D. Matignon, "Stability results for fractional differential equations with applications to control processing," *Comput. Eng. Sys. Appl.* vol. 2, no. 1, pp. 963–968, 1996.

[65] C. Li and Y. Ma, "Fractional dynamical system and its linearization theorem," *Nonlinear Dynamics*, vol. 71, no. 4, pp. 621–633, 2013.

[66] A. S. Shaikh, I. N. Shaikh, and K. S. Nisar, "A mathematical model of COVID-19 using fractional derivative: outbreak in India with dynamics of transmission and control," *Advances in Difference Equations*, vol. 2020, no. 1, pp. 373–419, 2020.

[67] P. Kumar, V. S. Erturk, and M. Murillo-Arcila, "A new fractional mathematical modelling of COVID-19 with the availability of vaccine," *Results in Physics*, vol. 24, Article ID 104213, 2021.

[68] M. Mohammad and A. Trounev, "On the dynamical modeling of COVID-19 involving Atangana-Baleanu fractional derivative and based on Daubechies framelet simulations," *Chaos, Solitons & Fractals*, vol. 140, Article ID 110171, 2020.

[69] A. A. M. Arafa, M. Khalil, and A. Sayed, "A non-integer variable order mathematical model of human immunodeficiency virus and malaria coinfection with time delay," *Complexity*, vol. 2019, pp. 1–13, 2019.

[70] A. M. A. El-Sayed, A. A. M. Arafa, M. Khali, and A. Sayed, "Backward bifurcation in a fractional order epidemiological model," *Progress in Fractional Differentiation and Applications*, vol. 3, no. 4, pp. 281–287, 2017.

[71] A. A. M. Arafa, S. Z. Rida, and M. Khalil, "A fractional-order model of HIV infection: numerical solution and comparisons with data of patients," *International Journal of Biomathematics*, vol. 07, no. 04, Article ID 1450036, 2014.

[72] A. Ali, M. Y. Khan, M. Sinan et al., "Theoretical and numerical analysis of novel COVID-19 via fractional order mathematical model," *Results in Physics*, vol. 20, Article ID 103676, 2021.

[73] P. Kumam, A. Ali, K. Shah, and R. A. Khan, "Existence results and Hyers-Ulam stability to a class of nonlinear arbitrary order differential equations," *The Journal of Nonlinear Science and Applications*, vol. 10, no. 06, pp. 2986–2997, 2017.

[74] H. Ramos, "Formulation and analysis of a class of direct implicit integration methods for special second-order IVPs in predictor-corrector modes," in *Recent Advances in Differential Equations and Applications*, pp. 33–61, Springer, Berlin, Germany, 2019.

[75] Worldometers, "Worldometers," 2022, https://www.worldometers.info/world-population/pakistan-population.

[76] Coronatracker, "Coronatracker," 2021, https://www.coronatracker.com/country/pakistan/.

[77] Current Information, "Current information about COVID-19 in Pakistan," 2021, https://www.worldometers.info.

[78] K. Shah, T. Abdeljawad, and R. Ud Din, "To study the transmission dynamic of SARS-CoV-2 using nonlinear saturated incidence rate," *Physica A: Statistical Mechanics and Its Applications*, vol. 604, Article ID 127915, 2022.